

# Porous Materials with Ultralow Optical Constants for Integrated Optical Device Applications

Hsuen-Li CHEN\*, Chung-I HSIEH<sup>1</sup>, Chao-Chia CHENG<sup>2</sup>, Chia-Pin CHANG<sup>2</sup>, Wen-Hau HSU,  
Way-Seen WANG and Po-Tsun LIU<sup>1</sup>

National Taiwan University, Taipei, Taiwan

<sup>1</sup>National Nano Device Lab., 1001-1 Ta Hsueh Road, Hsinchu, Taiwan

<sup>2</sup>Chung Hua University, Hsinchu 300, Taiwan

(Received October 27, 2004; accepted January 31, 2005; published July 26, 2005)

Ultralow dielectric constant ( $<2.0$ ) porous materials have received much attention as next-generation dielectric materials. In this study, optical properties of porous-methyl-silsesquioxane(MSQ)-like films (porous polysilazane, PPSZ) were characterized for optical waveguide devices applications. Measured results indicate that the refractive index is decreased to approximately 1.320 as the hydration time exceeds 24 h. The measured refractive index is about 1.163 at a wavelength of 1550 nm. PPSZ films have low absorption in the 500 to 2000 nm wavelength regime. Because of their relatively low refractive index and low absorption over a large spectral regime, PPSZ films can be good cladding materials for use in optically integrated devices with many high-refractive-index materials such as silicon oxide, silicon nitride, silicon, and polymers. We demonstrate two structures, ridge waveguides and large-angle Y-branch power splitters, composed of PPSZ and SU8 films to illustrate the use of low dielectric constant (K) cladding materials. The simulation results indicate that the PPSZ films provide better confinement of light. Experimentally, a large-angle Y-branch power splitter with PPSZ cladding can be used to guide waves with the large branching angle of  $33.58^\circ$ . [DOI: 10.1143/JJAP.44.5673]

KEYWORDS: low dielectric constant materials, porous films, porous polysilazane (PPSZ), ridge waveguides

## 1. Introduction

As the size of semiconductor devices shrinks, the low-dielectric constant (K) materials become a more important and critical issue.<sup>1)</sup> For 45 nm nodes, the dielectric constants of insulators should be below 2.1. Various low-K materials have been demonstrated and tested for both the electrical properties and the process compatibilities.<sup>1,2)</sup> Recently, ultralow-dielectric-constant ( $K < 2.0$ ) porous materials have received much attention as next-generation dielectric materials.<sup>3–5)</sup>

In addition to the fabrication of electrical devices, state-of-the-art semiconductor technologies are also useful for applications in integrated optical devices. The fabrication process for optical integrated circuits primarily follows those in semiconductor technology. Therefore, the study of materials used in integrated-circuit (IC) processes for integrated optical device fabrication is essential. On the basis of previous developments in low-K materials and technologies, new optical device structures may be developed and enhanced by combining them with low-K materials.

An important issue in integrated optical device applications is the coupling with optical fibers. Since glass fibers have relatively low refractive indices, the core layers of integrated optics must be as low as those of the fibers to avoid insertion loss due to refractive index differences. From this point of view, cladding layers need materials with even ultralow refractive indices to provide the light confinement and to enhance coupling efficiencies.<sup>6)</sup> Figure 1(a) shows the working principle of a three-layer waveguide, which is the simplest and most basic optical device structure. Since the guided electromagnetic waves are confined in the core layer due to total internal reflections, increases in refractive index differences between the core layer and the cladding layer would provide more incident light coupled into the core

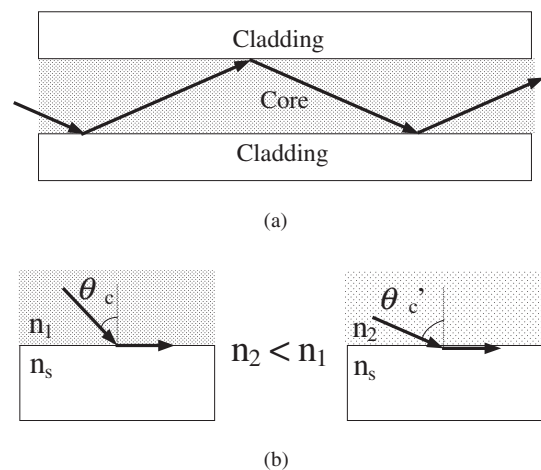


Fig. 1. (a) Scheme for propagation in a three-layer slab waveguide, and (b) the different core refractive indices and their corresponding critical angles.

region, as shown in Fig. 1(b). For this purpose, the use of porous materials is suitable to achieve high coupling efficiencies. One potential low-K material is porous polysilazane (PPSZ), which is a porous-methyl-silsesquioxane(MSQ)-like material with an ultra low dielectric constant. It may be a potential cladding material. In this study, optical characteristics of PPSZ films were measured for optical waveguide device applications.

In §2, the fabrication and mechanism of PPSZ films are discussed. Furthermore, optical properties and other thin film characteristics are also presented. In §3, we analyze waveguides with traditional claddings and PPSZ films by using the measured optical constants presented in §2. Furthermore, we fabricated a Y-branch power splitter with PPSZ claddings and measured its corresponding fields and efficiencies.

\*E-mail address: hsuenlichen@ccms.ntu.edu.tw

2. Fabrication and Properties of PPSZ Films

For this study, PPSZ was obtained from Clariant Inc. The fabrication process for PPSZ films can be divided into 3 steps.<sup>5)</sup> First, PPSZ precursors are spun on Si substrates at 2000rpm for 30 s by a spin coater. This followed by soft-baking steps at 150 and 280°C for 3 min to remove solvent. Second, the coated wafers were treated by hydration at different times from several hours to several days. During the hydration step, there are two mechanisms, hydrolysis and condensatio, by which the polymer structure is transformed into porous MSQ.<sup>4,5)</sup> Various hydration times can be used to change the porosities of PPSZ films. Subsequently, the wafers are cured in a quartz furnace at 400°C for 30 min with N<sub>2</sub> purging. The mechanism of PPSZ formation is shown in Fig. 2.

Reflection and transmission spectra of the PPSZ films were measured using a UV-visible-near-IR spectrometer (Hitachi U-4100). The measured spectra are plotted in Fig. 3(a). PPSZ provides very good transmission for wavelengths above 400 nm and without obvious absorption. The reflection and transmission spectra can be used to obtain the refractive index of PPSZ. As mentioned above, hydration time can be used to control the decrease in refractive indices

due to different degrees of porosity. As shown in Fig. 3(b), the pores in PPSZ become saturated after 24 h of hydration. The refractive index at 1.55 μm can be obtained using thin-film theory.<sup>7)</sup> From Fig. 3(a), the reflection and the transmission of the PPSZ film are 5.4% and 93.6%, respectively, and the corresponding refractive index,  $n_{\text{PPSZ}@1.55\mu\text{m}}$ , is 1.162.

The porosities can be obtained from the Maxwell-Garnett effective medium model.<sup>8)</sup> For a mixed film of two materials, the effective refractive index takes in the following form:

$$n_{\text{eff}} = \sqrt{\frac{n_{\text{MSQ}}^2(1 + 2q)/(1 - q) + 2n_{\text{air}}^2}{n_{\text{MSQ}}^2 + n_{\text{air}}^2(2 + q)/(1 - q)}} \quad (1)$$

Where  $n_{\text{eff}}$ ,  $n_{\text{MSQ}}$  and  $n_{\text{air}}$  are the optical constants of PPSZ, MSQ and air, respectively, and  $q$  is the volume fraction of the air holes. By inserting  $n_{\text{eff}}$  obtained in Fig. 3(b), porosities can be plotted as shown in Fig. 3(c). On the basis of the figure, the saturated PPSZ films with sufficient hydration may include more than 25% air holes which decrease the corresponding optical constants. PPSZ films with stable optical properties are shown in Fig. 3(d). To obtain the data in this figure, samples with different porosities are stored in the air. Fully hydrated samples have very small refractive index changes (within 1.6%). Porous materials usually suffer serious moisture penetration problems, which degrade the materials properties. The slight increase in the refractive indices may be due to the penetrated moisture, but such minor damage can be managed by careful design. By measuring the contact angles of the PPSZ films, the surface adhesion can be characterized. The measured data are listed in Table I. For PPSZ without any treatment, the contact angle of a water drop is 98.2°. This means the surface is water resistant, and this property can be used to explain the stability of PPSZ films. This water resistance property can also be useful for optical packaging applications. On the other hand, oxygen plasma treatment decreases the relative contact angle.

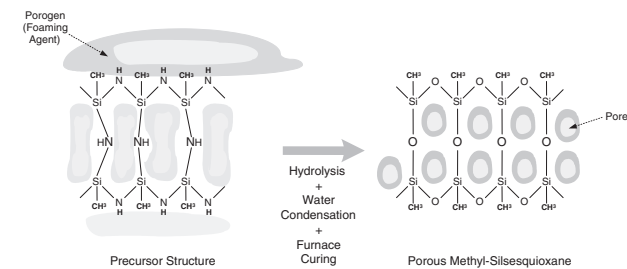


Fig. 2. Scheme for the change in precursor structure to porous-polysilazane (PPSZ) structure.

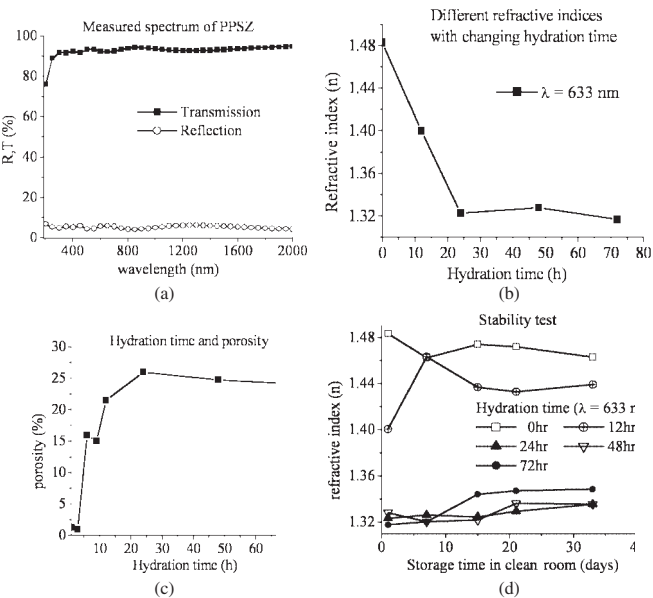


Fig. 3. (a) Spectra of PPSZ films, (b) the hydration times and their corresponding refractive indices, (c) the porosities, and (d) duration test of PPSZ films.

3. Ridge Waveguides and Related Applications with PPSZ Claddings

Since the refractive index of PPSZ films is relatively low ( $n_{@1.55\mu\text{m}} = 1.162$ ), more properties can be examined by realizing a waveguide. Figure 4 shows the structure of a ridge waveguide, which is based on the three-layer slab waveguide as shown in Fig. 1 with the addition of  $x$ -directional confinement. The upper cladding is air, the refractive index of which is 1.0, and the lower cladding is a material with a low optical constant.

Another issue is the core material, for which we choose SU8 because of its easy fabrication without the need for any other thin-film or etching process.<sup>9)</sup> Moreover, such polymer-based waveguides with lower optical constants (com-

Table I. List of contact angles of water drops on PPSZ films.

Contact angles of water drops	
PPSZ without any treatment	98.2°
PPSZ after O <sub>2</sub> plasma treatment	12.3°

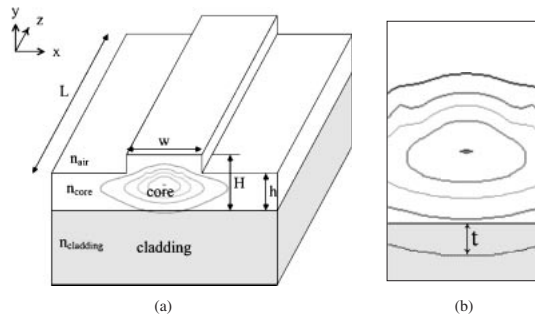


Fig. 4. (a) Scheme for the ridge waveguide and (b) the enlarged plot of waveguide modes.

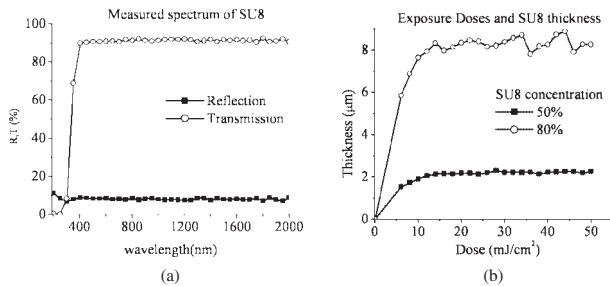


Fig. 5. (a) Measured spectrum and (b) sensitivity curves from e-beam exposure of SU8.

pared with III-V compounds or silicon) can decrease the insertion loss during connection with optical fibers. As we demonstrate for the SU8 polymer waveguide in this study, various polymers are compatible with PPSZ claddings.<sup>10)</sup>

Before simulations and experiments, the optical constants and process parameters of SU8 must be determined. Optical spectra are shown in Fig. 5(a), and the calculated refractive index,  $n_{\text{SU8}@1.55\mu\text{m}}$ , is 1.583. Epoxy-based SU8 resists have been widely used in MEMS processes. Figure 5(b) shows the sensitivity curves of SU8 resists during electron beam exposure at different concentrations. The SU8 ridge height and slab thickness can be easily controlled by changing exposure dosage distributions without the need for etching processes.

The geometries of ridge waveguides can be designed by the effective index method.<sup>11)</sup> The calculated ridge height ( $H$ ), slab height ( $h$ ) and ridge width ( $w$ ) are  $H = 0.75\mu\text{m}$ ,  $h = 0.5\mu\text{m}$ , and  $w = 1\mu\text{m}$ , respectively. The refractive indices of fused silica, PPSZ, and SU8 are 1.45, 1.162, and 1.583, respectively. The propagation mode of the PPSZ cladding ridge waveguide with these geometries is shown in Fig. 4. The asymmetric mode shape along the  $y$ -direction is primarily due to the differences between the indices of air and the lower cladding materials. Both geometric designs and lower index claddings can enable the mode symmetry to be modified. Figure 4(b) shows the field penetrating into the cladding layers. The field penetration depth can also be controlled by changing the index difference between the core and cladding materials. Ideally, air should be the lowest-index cladding material to achieve perfect symmetry. Using PPSZ and other materials with ultralow refractive indices can decrease the asymmetry.

The beam propagation method is also useful for examin-

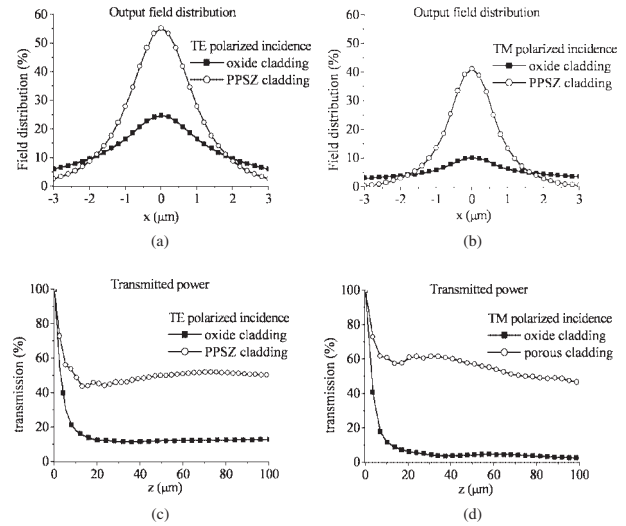


Fig. 6. (a), (b) Simulated field distributions and (c), (d) the corresponding transmitted power of PPSZ-cladding ridge waveguides in different polarization cases.

ing the performance of waveguides.<sup>7)</sup> Figures 6(a) and 6(b) show the simulated output field distributions of the ridge waveguides with different cladding materials of different polarized incidences for a  $100\mu\text{m}$  guiding distance. In both polarized incidences, PPSZ cladding provided better guided power, and the enhancement factors were 2.7 and 5 for TE and TM cases, respectively. Not only are the peaks of guided waves enhanced but values of the full width at half maximum (FWHM) are also improved in PPSZ claddings. Figures 6(c) and 6(d) show the transmitted power in the propagating direction ( $z$ ). Note that the transmissions along fused silica claddings are stabilized rapidly, whereas the transmission distribution of the PPSZ-clad waveguides still varies along the  $100\mu\text{m}$  distances. This shows that the more guided modes are confined in the core region and provide multimode interferences. Multimode coupling and formation may be useful for achieving highly efficient coupling devices or wavelength division multiplexers (WDM).

To qualitatively verify the performance of the waveguide described above, we devised a Y-branch power splitter scheme using our previously reported design.<sup>12)</sup> The schematic plot of such a Y-branch structure is shown in Fig. 7(a). Traditionally, such a device composed of two curved waveguides is not designed with a large branching angle because of power loss considerations. The longer distance between two output waveguides and shorter turning distance would cause more serious power loss and the output signals

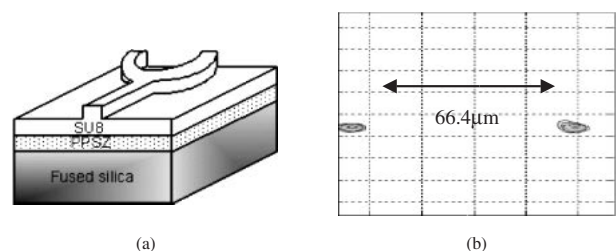


Fig. 7. (a) Scheme of Y-branch power splitter and (b) the measured field distributions.

would easily be lost. From the literature, the effective full branching angle is  $19.7^\circ$ . For our fabricated Y-branch waveguide including low-K cladding materials, the turning distance  $L_{\text{off}}$  of  $110\text{ }\mu\text{m}$  and the distance between two output waveguides  $X_{\text{off}}$  of  $66.4\text{ }\mu\text{m}$  are set. According to this design, a large branching angle of  $33.58^\circ$  can be obtained by using the film structure as shown in Fig. 7(b).

#### 4. Conclusions

Since low-K materials such as spin-on polymers provide low dielectric constants and good compatibilities with standard semiconductors, their optical properties may be suitable for integrated optics. One potential ultralow-K material, PPSZ, which is a porous-MSQ-like film, was tested and characterized for its optical property and stabilities. Such PPSZ films with relatively low refractive indices and absorption in the visible and near-IR regimes can be useful materials in many optical applications. The porosities of such polymers can be modulated by changing the hydration time, and the maximum porosities of PPSZ can reach 25% according to optical measurements and analysis. Being waterproof is another good property of PPSZ. Ridge waveguides with PPSZ claddings provide highly efficient power transmission. However, due to the large index contrast, multimodes exist and interfere along the propagat-

ing direction. Such an efficient structure can be applied in Y-branch power splitters. Even if the designed effective branching angle is larger than  $30^\circ$ , the transmitted light can still be measured experimentally.

- 1) Semiconductor Industry Association, International Technology Roadmap for Semiconductor 2003 Updated (SIA Publication, 2003).
- 2) T. Hasegawa: Int. Electron Devices Meet. (1999) 623.
- 3) T. C. Chang, Y. S. Mor, P. T. Liu, T. M. Tsai, C. W. Chen, Y. J. Mei and S. M. Sze: J. Electrochem. Soc. **149** (2002) F81.
- 4) M. Padovani, L. Rhodes, S. A. B. Allen and P. A. Kohl: J. Electrochem. Soc. **149** (2002) F161.
- 5) T. C. Chang, T. M. Tsai, P. T. Liu, C. W. Chen, S. T. Yan, H. Aoki, Y. C. Chang and T. Y. Tseng: Thin Solid Films **447–448** (2004) 524.
- 6) K. Okamoto: *Fundamentals of Optical Waveguides* (Academic Press, New York, 2000).
- 7) H. A. Macleod: *Thin-film Optical Filters*, 3rd ed. (IOP publishing Ltd, Bristol and Philadelphia, 2001).
- 8) L. Ward: *The Optical Constants of Bulk Materials and Films*, 2nd ed. (IOP publishing Ltd, Bristol and Philadelphia, 1994).
- 9) SU8 in trademark of MicroChem Co.
- 10) L. Eldada and L. W. Shacklette: IEEE J. Sel. Top. Quantum Electron. **6** (2000) 54.
- 11) T. Tamir: *Guided-Wave Optoelectronics* (Springer-Verlag, Berlin, 1988).
- 12) C. W. Hsu, H. L. Chen and W. S. Wang: IEEE Photon. Technol. Lett. **15** (2003) 1103.